

## Reactions of $^{237}\text{Np}$ with $^4\text{He}$ near the interaction barrier\*

S. Y. Lin and John M. Alexander

*Department of Chemistry, State University of New York at Stony Brook, Stony Brook, New York 11794*

(Received 4 February 1977)

Cross sections have been measured for the reactions  $^{237}\text{Np}(^4\text{He}, f)$ ,  $(^4\text{He}, n)$ ,  $(^4\text{He}, 2n)$  at energies below the interaction barrier (17.5–22.5 MeV). The total reaction cross sections have been fitted to an equation for theoretical barrier penetration and parameters describing the interaction barrier have been obtained.

[ NUCLEAR REACTIONS, FISSION  $^{237}\text{Np}(^4\text{He}, f)$ ,  $(^4\text{He}, n)$ ,  $(^4\text{He}, 2n)$ ;  $E = 17.5\text{--}22.5$  MeV; measured  $\sigma(E)$ . ]

### I. INTRODUCTION

The primary purpose of this work is the determination of excitation functions for the reactions  $^{237}\text{Np}(^4\text{He}, f)$ ,  $(^4\text{He}, n)$ , and  $(^4\text{He}, 2n)$  at energies near and below the interaction barrier. Experimental measurements for this reaction system have been made previously by Fleury *et al.*<sup>1</sup> and Lessler *et al.*<sup>2</sup> Their work was mainly directed at energies greater than the interaction barrier. Only a very few measurements were made at energies below the barrier; this gave only a vague description of the excitation functions at low energies. Because of the obvious experimental difficulties associated with low cross sections and their rapid energy dependence, only very few reaction systems have been studied in this low energy region. Theoretical calculations have been very successful as a basis for the correlation of the reaction cross sections at higher energies (higher than the interaction barrier). However, they often disagree with experimental results at lower energies. This failure may well be due to the scarcity of experimental data that address the following aspects: (1) determination of details of the shape of the interaction barrier, and (2) the energy dependence of fission decay rates.

An attempt to systemize the experimentally determined reaction cross sections and their associated interaction barriers has recently been made by Vaz and Alexander.<sup>3</sup> In this study the real potential was taken to be parabolic at its maximum and hence the characteristic parameters are barrier height  $E_0$ , radius  $R_0$ , and curvature  $\hbar\omega_0$ .<sup>4</sup> The empirically extracted barrier heights and radii follow clear systematic trends and therefore they can be used to predict total reaction cross sections for energies close to and greater than the barrier. There are, however, not enough experimental data to allow systematization of these parameters with enough precision to be useful for energies below the bar-

rier. Local parameters rather than systematics are therefore pursued in this study of the reaction system  $^{237}\text{Np} + ^4\text{He}$ .

Another concern in this low energy region is the sensitivity of the fission width  $\Gamma_f$  and neutron width  $\Gamma_n$  to the excitation energy. Theoretical calculations of the competition between fission and neutron emission have been pursued for many years. These calculations have been rather unsuccessful presumably due to the requirement for a detailed knowledge of the properties of the nucleus in the very deformed saddle point configuration.<sup>5</sup> One can approach this problem by trying to obtain for each different fissile nucleus a semiempirical relationship for the energy dependence of  $\Gamma_f/\Gamma_n$  (or  $\Gamma_f/\Gamma_{\text{total}}$ ) that can account for the experimental results.<sup>6</sup> Such functions can then be used to test theoretical models for the level densities of nuclei in the saddle point configuration.

The purpose of this study is to strengthen our experimental knowledge of the reactions  $^4\text{He} + ^{237}\text{Np}$ , in order to gain a better understanding of both the interaction barriers and the fission competition.

### II. EXPERIMENTAL PROCEDURES

Neptunium ( $^{237}\text{Np}$ ) targets were irradiated at the Stony Brook FN tandem Van de Graaff accelerator by  $^4\text{He}$  with energies 17.5 to 22.5 MeV. The cross sections were measured for fission and for the reactions  $(^4\text{He}, n)$  and  $(^4\text{He}, 2n)$ . The method of Price and Walker<sup>7</sup> for the detection of fission fragments was employed. In this method strips of mica are used to detect the fission fragments. The tracks produced by fission fragments become easily visible under an ordinary microscope after the mica is treated with hydrofluoric acid. Tracks from particles of mass number  $\approx 30$  are not visible. The spallation products  $^{240}\text{Am}$  and  $^{239}\text{Am}$  were separated radiochemically<sup>8</sup> and then analyzed quantitatively by  $\gamma$ -ray spectroscopy.

### A. Activation of targets

Targets of  $^{237}\text{Np}$  with thickness ranging from 50–300  $\mu\text{g}/\text{cm}^2$  were prepared by electroplating Np on Ni foil ( $\approx 5 \text{ mg}/\text{cm}^2$ ). Target thicknesses were determined by absolute measurement of the  $\alpha$  radiation from  $^{237}\text{Np}$  with a Si(Li) surface barrier detector. The track detectors for fission products were rectangular strips of mica (1.2 cm by 2.8 cm) of thickness  $\approx 10^{-2}$  cm. The strips were cleaved along layer planes in order to get a fresh surface. Each strip was preetched with 46% hydrofluoric acid for two hours at room temperature, then washed with water and dried in the air. The exposures were carried out in a 76.2 cm scattering chamber with the target at  $45^\circ$  to the beam direction. Two track detectors (mica strips) were mounted 18.6 cm away from the target at angles of  $120^\circ$  and  $150^\circ$  with respect to the beam direction. In order to observe the fission tracks as lines in the detectors (rather than as pits) the mica strips were inclined at  $60^\circ$  with respect to the target surface. A schematic diagram is shown in Fig. 1. Three thin copper foils ( $\approx 2 \text{ mg}/\text{cm}^2$ ) were stacked behind the neptunium target as monitors of the beam intensity. Cross sections were determined at low energies (down to 15 MeV) for the monitor reactions  $^{63}\text{Cu}(^4\text{He}, 2n)^{65}\text{Ga} + ^{63}\text{Cu}(^4\text{He}, pn)^{65}\text{Zn}$  in a separate set of measurements made at the Stony Brook tandem Van de Graaff accelerator (see the Appendix). The beam energy for each foil was calculated from the incident energy and energy loss tables of Northcliffe and Schilling.<sup>9</sup>

The energy of the helium ion beam is determined by the terminal voltage and analyzing magnet with a precision of  $\pm 0.02\%$ . Two collimators with

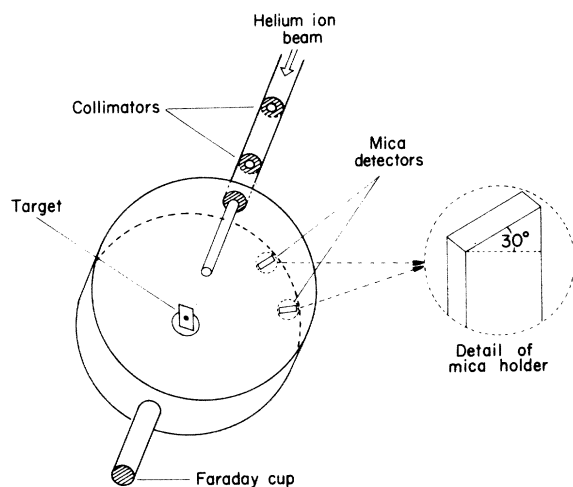


FIG. 1. Schematic drawing of the target and detector assembly.

apertures of 0.32 cm were used to locate the beam. After traversing the target the beam entered a Faraday cup connected to a current integrator. The integrator gave a second determination of the total number of incident particles. Beam intensities were limited to  $\leq 1 \mu\text{A}$  to avoid melting the targets. Each irradiation lasted about 8 to 10 hours.

### B. Radiochemical measurements

After bombardment the targets and backings were dissolved in 6 *M*  $\text{HNO}_3$  solution and added to a column of AG  $1 \times 10$  anion-exchange resin to remove nickel. Americium in the eluate was coprecipitated on  $\text{La}(\text{OH})_3$  in the presence of Zr holdback carrier, reprecipitated as  $\text{LaF}_3$ , and then again as  $\text{La}(\text{OH})_3$ . The resulting precipitate was dissolved in a minimum amount of saturated HCl solution and passed through a Dowex-50  $\times 12$  cation-exchange column, which was then eluted with concentrated HCl solution. The americium band was collected and evaporated to dryness on a hot platinum foil.<sup>8</sup> The entire separation took about two hours; all samples were essentially free of fission products, plutonium, and neptunium. The final sample was subsequently analyzed by  $\gamma$ -ray spectroscopy with a Ge(Li) detector of resolution  $\approx 2.7 \text{ keV}$ .

The  $\gamma$  rays of interest and their abundances are given in Ref. 1; detection efficiencies were calibrated with standard sources. Chemical yields were determined to be 30 to 40% by measurement of a  $^{241}\text{Am}$  "spike."

### C. Optical scanning of the fission tracks

After the irradiation, the mica strips were etched in 46% hydrofluoric acid for about 20 minutes, and scanned with a microscope. A number of fields of view along the center of the strip was scanned. As the beam energy is very near the Coulomb barrier we have assumed that fission is isotropic in the moving frame. Larger areas had to be scanned for the lower incident energies, because the density of tracks was only about 1 to 5 tracks per field of view ( $0.0009 \text{ cm}^2$ ).

## III. RESULTS AND DISCUSSION

### A. Spallation cross sections

The measured cross sections for fission and the production of  $^{240}\text{Am}$  and  $^{239}\text{Am}$  are listed in Table I. These cross sections along with those from Ref. 1 are shown in Fig. 2. Some of the measurements reported here overlap those reported previously.<sup>1</sup> In all cases but one the agreement is good; our result for the fission cross section at 19.5 MeV is

TABLE I. Cross sections for reactions of  $^{237}\text{Np}$  with  $^4\text{He}$  (mb).

Bombarding energy (MeV) (lab)	$(^4\text{He}, f)$	$(^4\text{He}, n)$	$(^4\text{He}, 2n)$	$\sum_1^2 \sigma_{xn}$	$\sigma_{\text{total}}$
17.5 (1) <sup>a</sup>	0.058	$\approx 0.004^c$			0.062
18.0 (2)	$0.17 \pm 0.06^b$	$\approx 0.016^c$			0.19
18.5 (1)	0.47	0.15	0.003	0.15	0.62
19.0 (2)	$1.20 \pm 0.14$	$0.32 \pm 0.06$	$0.030 \pm 0.001$	0.35	1.55
19.5 (1)	1.84	0.44	0.077	0.52	2.36
20.0 (1)	3.60	0.42	0.14	0.56	4.17
20.5 (1)	8.86	0.79	0.44	1.23	10.1
21.0 (3)	$17.1 \pm 1.0$	$1.03 \pm 0.16$	$0.98 \pm 0.20$	2.00	19.1
21.5 (2)	$25.6 \pm 2.6$	1.25	1.78	3.03	31.3
22.0 (3)	$54.3 \pm 9.0$	$0.99 \pm 0.01$	$2.06 \pm 0.13$	3.05	57.4
22.5 (1)	100.7	1.24	3.98	5.51	106

<sup>a</sup>Number of determinations.

<sup>b</sup>Uncertainties are standard deviations.

<sup>c</sup>Activities were very low and these results are thus more subject to systematic errors in background subtraction.

much greater than that of Ref. 1. This difference is due to the monitor cross section used. This is discussed in the Appendix. A detailed comparison of these results to evaporation calculations is made in the accompanying paper.<sup>10</sup> Our discussion here is restricted to comparisons with earlier work.

The general features of the excitation functions for spallation reactions in  $^{237}\text{Np}$  are similar to those for other very heavy elements.<sup>11-13</sup> As we see from Fig. 2 the cross section for the  $(^4\text{He}, n)$  reaction dominates for energies less than 21 MeV. At higher energies the  $(^4\text{He}, 2n)$  reaction peaks at about 25 mb followed by the  $(^4\text{He}, 3n)$  reaction at

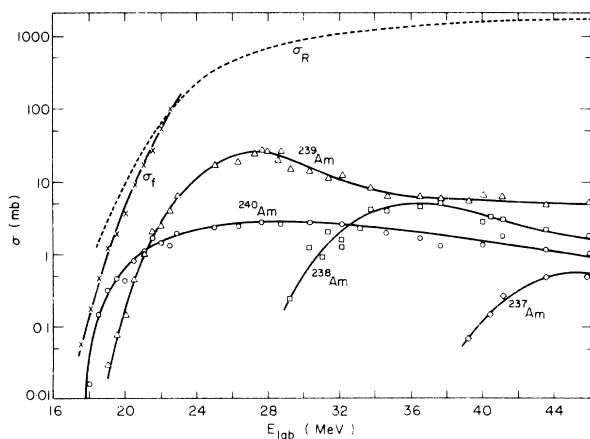


FIG. 2. Cross sections as a function of energy for products from the bombardment of  $^{237}\text{Np}$  with 17.5–45 MeV  $^4\text{He}$ . Points at energies higher than 23 MeV were taken from Ref. 1. Solid lines are hand fits to the data points. The dashed line for  $\sigma_R$  was calculated by the optical model (Ref. 14).

about 5 mb and then  $(^4\text{He}, 4n)$ . This trend is typical of the excitation functions for the  $(^4\text{He}, xn)$  reactions (for  $x$  greater than 1); the peaks decrease in magnitude as  $x$  increases.<sup>11-13</sup> This decrease reflects the competition from fission at each step in the

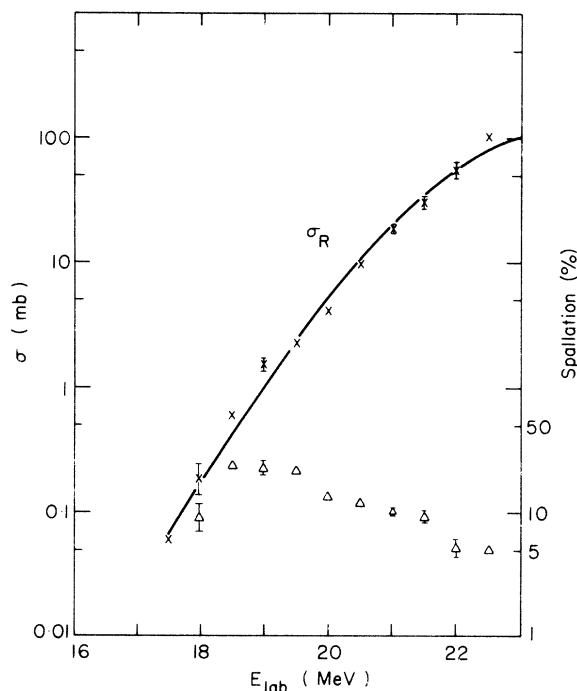


FIG. 3. Total reaction cross sections  $\sigma_R$  (left scale) and percentage of spallation (right scale) for the reaction  $^{237}\text{Np} + ^4\text{He}$ . The solid line is a fitted curve from Eq. (1) (see Table II):  $\times$ , reaction cross sections;  $\Delta$ , percent spallation.

TABLE II. Reaction cross sections (mb), calculated and measured.

Lab energy (MeV)	$\sigma_{\text{expt.}}$	$\sigma_{\text{calc.}}^{\text{a}}$	$\sigma_{\text{calc.}}^{\text{b}}$
17.50	0.062	0.103	0.072
18.00	0.19	0.217	0.171
18.50	0.62	0.46	0.41
19.00	1.55	0.96	0.95
19.50	2.36	2.01	2.18
20.00	4.17	4.17	4.84
20.50	10.1	8.5	10.1
21.00	19.1	17.0	19.4
21.50	31.3	32.3	33.7
22.00	57.4	57.4	53.6
22.50	106.	94.5	79.2

<sup>a</sup>Two free parameter search:  $r_0$  (1.41 fm),  $\hbar\omega_0$  (4.00 MeV). Best fit parameters:  $\bar{E}_0=22.1$  MeV;  $\Delta=1.03$  MeV.

<sup>b</sup>Three free parameter search:  $r_0$  (1.41 fm). Best fit parameters:  $\bar{E}_0=23.1$  MeV;  $\Delta=3.20$  MeV,  $\hbar\omega_0=3.50$  MeV.

neutron evaporation chain.

A long tail is noted for the ( $^4\text{He}, xn$ ) excitation functions here as is typical for these reactions.<sup>13</sup> In addition the cross sections for the reactions involving the emission of charged particles are rather large for energies greater than 23 MeV. These facts suggest direct or preequilibrium reactions of the projectile with a few nucleons on the nuclear surface. When such direct interaction occurs, the initial excited compound nucleus is bypassed, with the result that fission has fewer chances to compete with particle emission than when the highly excited compound nucleus is formed. Thus the products from direct-interaction mechanisms often survive fission, whereas the products which are formed by evaporation of neutrons from a compound nucleus tend to be heavily suppressed by fission. Nevertheless, most cross sections for direct interactions have been shown to be small compared with those for fission plus neutron evaporation.<sup>13</sup>

TABLE III. Cross sections for  $^{63}\text{Cu}(^4\text{He}, 2n)^{65}\text{Ga} + ^{63}\text{Cu}-(^4\text{He}, pn)^{65}\text{Zn}$ .

Energy (MeV) (lab)	Ref. a (mb)	Ref. a (mb)	Ref. b (mb)	This work (mb)	Energy (MeV) (lab)	Ref. a (mb)	Ref. a (mb)	Ref. b (mb)	This work (mb)
46.0	310				22.5			820	
43.7	410				22.25				704
38.9	630				21.9		440		
38.1			520		21.17				613
38.0		700			21.1			540	
37.0		780			20.77				520
36.4	890				20.62				564
36.0		850			20.4	120			
35.0			920		20.3		250		
34.9		940			20.09				477
33.7		1050			19.93				391
33.6	1080				19.7			340	
32.5		1070			19.55				359
31.2		1090			19.08				293
30.5	1080				19.00				303
30.1		1050	1050		18.7		63		
29.0			1030		18.42				211
28.9		1070			18.2			110	
27.6	980		1020		17.81				156
27.5		950			17.32				88
26.5			1020		17.20				81
26.3		920			17.1			18	
25.2			1000		16.61				43
24.9		800			16.40				29
24.2	620				16.0	57			
23.9			920		15.97				15
23.5		660			15.46				3.9
23.27				920	15.35				3.1
22.76				770					

<sup>a</sup>F. H. Ruddy, (private communication); these two experiments were carried out on the BNL 60 in. cyclotron.

<sup>b</sup>F. H. Ruddy, Ph.D. thesis, Simon Fraser University, Burnaby, British Columbia, 1968 (unpublished).

### B. Total reaction cross sections

The total reaction cross section can be obtained by summing the experimental fission and spallation cross sections as listed in Table I. Optical model calculations from the ABACUS code are shown in Fig. 2 along with the measured values.<sup>14</sup> The percentage of spallation reactions compared with the total reaction cross section is also shown. Cross sections for reactions involving charged particle emission are neglected in this sum, but this omission is not expected to be serious for energies less than 23 MeV.

As pointed out by many authors<sup>3,15,16</sup> the optical model calculations have generally been fitted to the experimental results in the energy region greater than the interaction barrier. In the low energy region our results differ considerably from the calculations as shown in Fig. 2. The calculated values are significantly higher than the experimental results. This divergence strongly suggests the necessity of modifying the optical model parameters or the use of another approach to deal with the particular difficulties at low energies.

Vaz and Alexander<sup>3</sup> have pointed out the special problems associated with the calculation of the reaction cross sections at energies below the interaction barrier. The experimental values from this work have been fitted to the following expression<sup>3,4</sup>:

$$\sigma_{R_0}(E) = \int_{\bar{E}_0 - \Delta}^{\bar{E}_0 + \Delta} \frac{R_0^2}{2} \frac{\hbar\omega_0}{E} \ln \left[ 1 + \exp \left( \frac{2\pi(E - E_0)}{\hbar\omega_0} \right) \right] dE_0. \quad (1)$$

This expression results from a uniform spectrum of inverted parabolic barriers of height  $\bar{E}_0 - \Delta$  to  $\bar{E}_0 + \Delta$ , each with curvature  $\hbar\omega_0$ , and radial position  $R_0 = r_0(A_t^{1/3} + A_p^{1/3})$ . Two parameter searches were carried out. First, the values of  $r_0$  and  $\hbar\omega_0$  were fixed at 1.41 fm and 4.0 MeV, respectively; the best fit values of  $\bar{E}_0$  and  $\Delta$  were found to be 22.1 and 1.03 MeV, re-

spectively. In the second search, only the value of  $r_0$  was fixed (1.41 fm); the values of  $\bar{E}_0$ ,  $\Delta$ , and  $\hbar\omega_0$  were found to be 23.10, 3.2, and 3.5 MeV, respectively. Experimental and calculated cross sections are compared in Table II and Fig. 3. Very good fits are obtained in both cases. As pointed out previously,<sup>3</sup> however, these parameter sets are not general; they simply provide good fits to the data for the system,  $^{237}\text{Np} + ^4\text{He}$ . More data at low energies for different reaction systems are needed to generate the systematic behavior of the parameters  $\bar{E}_0$  and  $\Delta$ . Such data are available for reactions of  $^4\text{He}$  with  $^{208}\text{Pb}$ ,  $^{209}\text{Bi}$ , and  $^{233}\text{U}$  (Refs. 16 and 17); these results and those from this work have been used to explore one aspect of the reaction systematics—the role of static nuclear deformation. The discussion of this problem has been given in another paper.<sup>18</sup>

### APPENDIX: EXCITATION FUNCTION OF $^{63}\text{Cu}(^4\text{He}, 2n)^{65}\text{Ga} + ^{63}\text{Cu}(^4\text{He}, pn)^{65}\text{Zn}$

The excitation function for these reactions has been measured previously by Ruddy<sup>19</sup>; he used cyclotron beams. The measured cross sections are listed in Table III. In this study irradiations were made at the Stony Brook Van de Graaff accelerator for energies less than 24 MeV. They are normalized to the value at 24 MeV obtained by Ruddy. The cross sections obtained here at energies below 20 MeV are quite different from the earlier study. This is not unexpected and is probably due to uncertainties in the effective beam energy at low energies after extensive energy loss; the lowest external beam energy for helium ions at the Brookhaven 60 in. cyclotron is 34 MeV. The cross sections measured at the Stony Brook Van de Graaff accelerator are listed in the last column in Table II. As this is quite a useful beam monitor we tabulate the whole collection of data. We feel that the results from this work are more accurate for energies  $\lesssim 22$  MeV.

\*Work supported in part by the Atomic Energy Commission.

<sup>1</sup>A. Fleury, F. H. Ruddy, M. N. Namboodiri, and J. M. Alexander, Phys. Rev. C **7**, 1231 (1973).

<sup>2</sup>R. M. Lessler, W. M. Gibson, and R. A. Glass, Nucl. Phys. **81**, 401 (1966); W. M. Gibson, Lawrence Radiation Laboratory Report No. UCRL-3493, 1956 (unpublished).

<sup>3</sup>L. C. Vaz and J. M. Alexander, Phys. Rev. C **10**, 464 (1974).

<sup>4</sup>C. Y. Wong, Phys. Lett. **42B**, 186 (1972); **31**, 766 (1973).

<sup>5</sup>R. Vandenbosch and J. R. Huizenga, *Nuclear Fission* (Academic, New York, 1973).

<sup>6</sup>T. Sikkeland, Phys. Rev. **135**, B699 (1964). A. M.

Zebelman, L. Kowalski, J. Miller, K. Beg, Y. Eyal, G. Jaffe, A. Kandil, and D. Logan, Phys. Rev. C **10**, 200 (1974).

<sup>7</sup>R. L. Fleischer, P. B. Price and R. M. Walker, Annu. Rev. Nucl. Sci. **15**, 1 (1965).

<sup>8</sup>R. A. Penneman, Nuclear Science Report Series, No. NAS-NS 3006, 1960 (unpublished).

<sup>9</sup>L. C. Northcliffe and R. F. Schilling, Nucl. Data **A7**, 233 (1970).

<sup>10</sup>J. Gilat, A. Fleury, H. Delagrangé, and J. M. Alexander, following paper, Phys. Rev. C **16**, 694 (1977).

<sup>11</sup>R. Vandenbosch, T. D. Thomas, S. E. Vandenbosch, R. A. Glass, and G. T. Seaborg, Phys. Rev. **111**, 1358 (1958); R. A. Glass, R. J. Carr, J. W. Cobble, and

- G. T. Seaborg, Phys. Rev. 104, 434 (1956).
- <sup>12</sup>B. G. Harvey, A. Chetham-Strode, A. Ghirso, G. R. Choppin, and S. G. Thompson, Phys. Rev. 104, 1315 (1956).
- <sup>13</sup>E. K. Hyde, *The Nuclear Properties of the Heavy Elements III. Fission Phenomena* (Prentice-Hall, Englewood Cliffs, N. J., 1964).
- <sup>14</sup>Real well depth 50 MeV. Imaginary well depth 27 MeV. Interaction radius  $1.17A^{1/3} + 1.77$  fm. Well diffuseness 0.576 fm.
- <sup>15</sup>A. Fleury and J. M. Alexander, Annu. Rev. Nucl. Sci. 24, 279 (1974).
- <sup>16</sup>H. Freiesleben and J. R. Huizenga, Nucl. Phys. A224, 503 (1974).
- <sup>17</sup>A. R. Barnett and J. S. Lilley, Phys. Rev. C 9, 2010 (1974).
- <sup>18</sup>J. M. Alexander, L. C. Vaz, and S. Y. Lin, Phys. Rev. Lett. 33, 1487 (1974).
- <sup>19</sup>See footnotes to Table III.